Arch. Mech., 37, 4-5, pp. 321-336, Warszawa 1985

Modelisation of glass spinning

J. R. CLERMONT, J. M. PIERRARD and C. GODET (GRENOBLE)

TWO THEORETICAL models have been considered for the upper jet region of the molten glass during the fibre spinning process. The first model uses the experimental data of temperature and velocity measurements at the surface in the Navier–Stokes equations in order to determine the temperature field in the upper jet region. The second model is introduced to determine the approximate, physically reasonable values of the radiative flux vector as well as the convective transfer coefficient between the glass and its surroundings. These quantities may be used in a more advanced study of the problem

Rozważono dwa teoretyczne modele dla górnej części strugi stopionego szkła w procesie przędzenia włókna. Pierwszy model wykorzystuje doświadczalne pomiary temperatuty i prędkości na powierzchni w równaniach Naviera–Stokesa w celu określenia pola temperatury w górnej części strugi. Drugi model wprowadzono w celu określenia przybliżonych, fizycznie uzasadnionych, wartości strumienia radiacyjnego jak również współczynnika konwekcyjnego przenoszenia między szkłem i jego otoczeniem. Wielkości te mogą być wykorzystane w bardziej zaawansowanych badaniach.

Рассмотрены две теоретические модели для верхней части струи сплавленного стекла в процессе прядения волокна. Первая модель использует экспериментальные измерения температуры и скорости на поверхности в уравнениях Навье–Стокса с целью определения поля температуры в верхней части струи. Вторая модель введена с целью определения приближенных, физически обоснованных, значений радиального потока, как тоже коэффициента конвекционного переноса между стеклом и окружающей его средой. Эти величины могут быть использованы в более развитых исследованиях.

1. Introduction

THE PROCESSING of glass fiber which is involved particularly in textile and composite industry is related to strong temperature-dependent properties. In the present paper we analyze the formation of glass fiber in liquid state starting at high temperature (between 1300°C–1500°C) from a nozzle of approximately 0.2 cm in diameter. In Fig. 1 we give a schematic view of the flow domain from the orifice at $z = z_0 = 0$ to the solid flow

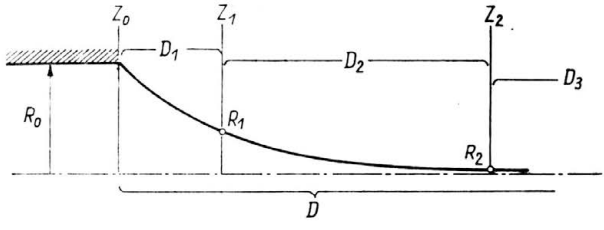

FIG. 1. Schematic diagram of the glass jet.

at $z = z_2$. The glass fiber has generally a diameter of 10–50 microns and is wounded up at a constant speed between 5 m/s to 60 m/s. In the industrial process, the fiber glass is obtained from draw plates of more than a thousand nozzles. We restrict ourselves to the case of one filament, which can provide an interesting and comprehensive stand-point for the study of the multi-filament process.

As shown in Fig. 1, three regions can be considered in the drawing flow field:

The upper region D_1, where the slope of the jet is large, and the radiative heat transfer is important due to the high temperature and physical properties of glass.

The central jet region D_2 is characterized by a uniform distribution of the axial velocity and a small slope of the free surface.

The constant radius jet region D_3, downstream from region D_2. The importance of the upper jet region and the central jet region is about fifteen to twenty radii of the nozzle, i.e. approximately 2 cm, what is much less than the fiber flow domain for polymer extrusion which is about 60 cm.

The process of glass fiber formation is, in some aspects, different from the polymer spinning, the drawing rates being of the same order.

1) The distance $z_2 - z_0$ is more important for the polymer fiber drawing and is about 50 cm.

2) The temperature in the drawing field between z_0 and z_2 is 1500°C – 700°C for the glass and 300°C – 50°C for polymers.

3) The broad range of temperature for the glass should be considered together with the strong viscosity variation (of the exponential type).

The strong dependence of glass properties on temperature in the relatively small domain lead to particular care when considering the glass spinning problem. The viscosity depends strongly on temperature (many authors consider it to be exponential), the radiative transfer is preponderant in the first millimeters of the jet (the upper region D_1), the velocity gradients are important and convective exchange is to be taken into account between the glass and it surroundings. The complete treatment of the glass fiber drawing problem in the liquid state must involve the conservative laws of mass, momentum and energy assorted with appropriate boundary conditions (in particular, the free surface is unknown) and realistic models for the rheological equation of glass and the radiative transfer.

2. Thermal problem

Approaching the thermal problem for glass, the material can be considered as a semi-transparent medium. The conduction can be characterized by the conduction vector:

$$\mathbf{q}_c = -k_c \mathbf{grad}\, T, \tag{2.1}$$

T is the temperature, k_c is the conduction coefficient.

For the radiation problem, the glass absorption coefficient versus the wavelength distribution is generally used, which leads to the definition of global quantities as the Rosseland's averaged absorption K_R given by the following equation:

$$\frac{1}{K_R} = \frac{\int_0^\infty \frac{1}{K_r} \frac{dI_\lambda^0}{dT} d\lambda}{\int_0^\infty \frac{dI_\lambda^0}{dT} d\lambda}, \tag{2.2}$$

where I_λ^0 is the Planck's function, λ the wavelength and the radiative conductivity coefficient k_r which is defined as follows:

$$k_r = \frac{16}{3} \frac{n^2 \sigma T^3}{K_R}, \tag{2.3}$$

where σ is the Stefan–Boltzmann coefficient, n is the relative index of the medium.

This coefficient enables to introduce the optical thickness concept which characterizes the nature of the radiative heat transfer in an absorbing medium of dimension L. The optical thickness τ is given by the equation

$$\tau = K_R \cdot L. \tag{2.4}$$

The medium under consideration is optically thick (optically thick medium) if we have:

$$\tau \gg 1. \tag{2.5}$$

This means that significant radiation occurs in short distances. The radiative heat flux vector can be written as

$$\mathbf{q}_r = -k_r \mathbf{grad}\, T, \tag{2.6}$$

and the total heat flux (conduction and radiation) can be written as:

$$\mathbf{q} = \mathbf{q}_c + \mathbf{q}_r = -(k_c + k_r)\, \mathbf{grad}\, T. \tag{2.7}$$

This case is similar to that of pure conduction.

When the optical thickness is

$$\tau \ll 1, \tag{2.8}$$

the medium is called optically thin and in that case the relevant heat transfer equation is not simple [1].

The textile glass generally used in fiber processing is *E*-glass which, according to recent studies at the Saint Gobain Company [2], is neither optically thin nor optically thick under the conditions of glass spinning process.

3. Previous work

In the literature several studies have been devoted to the glass spinning problem and, practically, all the papers refer to experimental data of GLICKMAN'S study, [3, 4, 5] which can be considered as the first important work to be pointed out. In his experiments, Glicksman measured the glass temperature by using an optical pyrometer which is subjected to radiation from the glass. These experimental data of temperature are actually the only ones to be used as control values for the numerical simulations proposed in the litera-

ture. In the following it will be shown that this method of temperature measurement is more affected by the radiation than a technique based on the use of a small-size thermocouple. Considering again Glickman's work, the author also investigated the glass fiber problem from the theoretical point of view. The analysis was particularly devoted to the central region D_2 of the jet which was assumed to begin at the value z_1 where the slope of the free surface is one-tenth or less, in absolute value. The study of glass in the central jet region gives more simplicity to the analysis because the velocity and temperature fields can be considered as being one-dimensional. Moreover, in this region, the radiation is less important in the upper region D_1 because of the lower temperature range. In Glicksman's work, the glass is assumed to be Newtonian, with a strongly temperature-dependent viscosity; for the radiation, GLICKSMAN used a step model [3].

A complete method for the solution of glass spinning problem was given by CASWELL and SAYLES [6]. These authors, using a finite element technique, have developed a theoretical model for the radiation inside the jet and a method for taking into account the convective transfer between the glass jet and the surrounding air. However, it is to be pointed out that the results of the model were compared with Glicksman's data of temperature. STEHLE and BRUCKNER [7, 8] presented an experimental and theoretical work on the glass-spinning problem, but the dynamical equations used in their model were related to the one-dimensional case and for the energy equation simplified relations were proposed. HUYNH and TANNER [9] have presented in a recent paper a computational analysis in the two-dimensional case with a finite element method, but it should be noticed that in the energy equations the radiative transfer was assumed to be governed only by the thermal exchange at the free surface. These equations involve an emissivity coefficient which was computed to match the Glicksman's data of the filament radius.

The points developed in the literature on the glass spinning problem can be summarized as follows:

1) The rediative heat transfer equation under the conditions of glass spinning is unknown and, as precised in Sect. 2, cannot be represented by a classical radiation model.

2) Measurements of temperature are obtained by optical techniques. Data from an optical pyrometer are subjected to radiation from the glass. Up to the present analysis, we are not aware of measurements of velocities in the glass jet, except for the drawing rate V_2.

3) The estimate of parameters involving the convective and radiative heat transfer between the glass and its surroundings should be considered with great care when using the boundary condition [6].

From these conclusions, it results that actually a realistic solution of the glass spinning problem cannot be obtained by considering the global conservation equations of state, mass and energy. The considerations previously made lead us to present a theoretical model which is based on some experimental and theoretical results. These data enable to set up a numerical model which uses only the conservation of mass and momentum equations, and avoids the difficulty of involving the radiation problem in the equations of energy and the delicate estimate of parameters in the boundary conditions. In this method, we use data of the filament radius, temperature and velocity at the jet surface, concerning the upper and central regions of the flow beyond the nozzle. The temperature data are

obtained with a termocouple of small size and short response time and the kinematics is measured with a laser velocimeter. The glass is an incompressible material which can be considered as a Newtonian fluid of viscosity which highly depends on temperature. In this paper we show that it is possible to determine in the glass jet, with the aid of experimental kinematic data and additional assumptions concerning the jet surface, the streamlines and the velocities in an analytical form. This is performed with the aid of a stream-function $H(\varrho, z)$. Then, when considering the Navier–Stokes equations, the kinematic terms are known and the experimental data of temperature at the free surface are used as the boundary conditions. The dynamical equations involve the isotropic pressure and the viscosity as unknowns. The numerical technique is carried out in the upper jet region and the temperature field in this region is calculated from the viscosity equation.

. Experimental

The flow of molten glass is performed by using a resistance-heated rhodium-platinum reservoir. The schematic picture of the fiber drawing is shown in Fig. 2. No pressure is applied in the reservoir. The jet diameter decreases very rapidly, and, apart from measure-

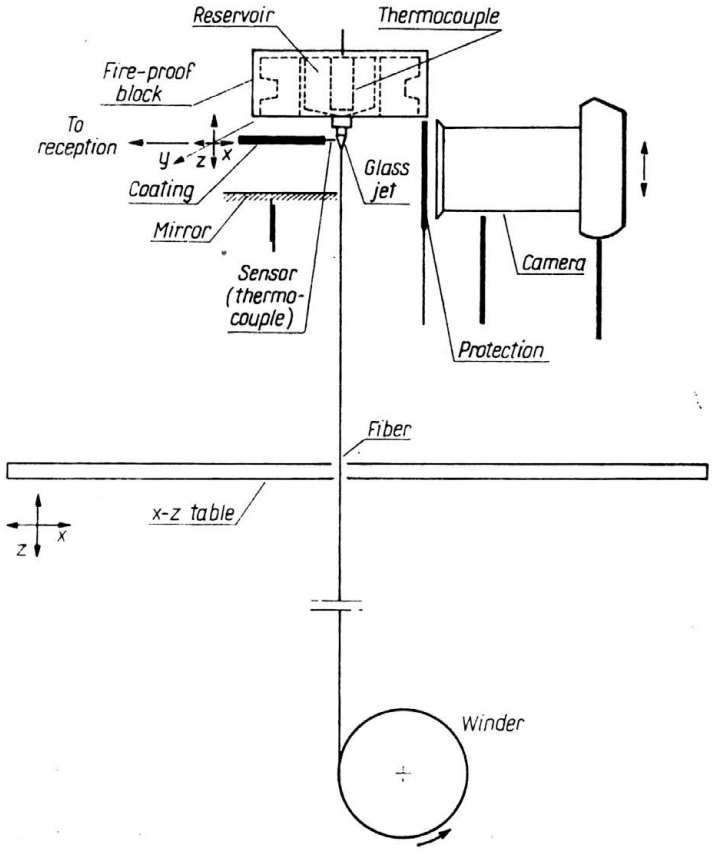

FIG. 2. Experimental set-up.

ments for the jet shape with a camera (and the control of the final radius R_2 of the fiber by using a microscope), we measure the drawing rate V_2, the reservoir temperature, the temperature at the free surface with a thermocouple and the velocities of points of the free surface by means of a laser velocimeter.

4.1. Velocity measurements

It was impossible to measure the velocities inside the bulb because of the high radiation in the upper jet region, the small size of the filament and the rapid decrease of the jet radius. We measured only the axial component v at the free surface of the upper zone with the aid of an Argon laser using a retrodiffusion method which avoided the crossing of the medium. The point of measurement was localized by optical means.

4.2. Temperature measurements

The use of a small-size thermocouple (total diameter 0.25 mm) for the temperature measurements in the liquid part of the jet was motivated by the reduction of radiation emitted from the glass to the sensor and the minimization of the flow perturbation at the vicinity of the surface point of measurement. Moreover, the response time was about 5 milliseconds. The positioning of the thermocouple was performed with a micrometric

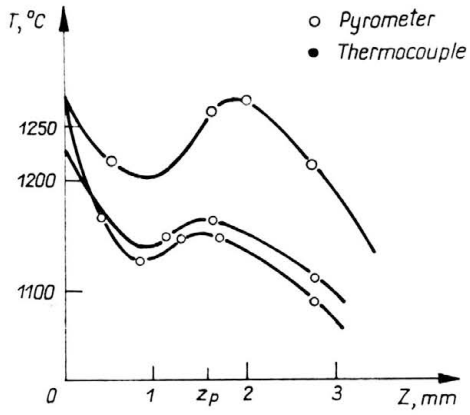

FIG. 3. Temperature at the free surface.

table and temperature measurements were obtained up to 6 mm (6 radii) downstream the exit section of the glass jet. The experiments permitted to define an optimal position of the axis of the thermocouple (normal to the jet axis). In Fig. 3, we give the temperature variations at the free surface versus z obtained by an optical pyrometer and the small size thermocouple. The local peak of the curves, for $z \gtrsim 1.5\ R_0$ is more important in the case of the optical pyrometer and, consequently, indicates that the smoothed curve deduced from the thermocouple measurement — the peak is due to radiation from the glass — is closer to the real temperature than that given by the optical pyrometer.

5. Theoretical model

According to the flow domain D shown in Fig. 1, we obtain the velocity field as

$$\mathbf{V} = u(\varrho, z) \cdot \mathbf{e}'_p + v(\varrho, z)\mathbf{e}'_z, \tag{5.1}$$

$(\mathbf{e}'_\varrho, \mathbf{e}'_\theta, \mathbf{e}'_z)$ is the orthonormal frame associated with the cylindrical coordinates $\varrho = 1$, $\theta = 2$, $z = 3$.

From the decomposition of domain D into three elementary zones D_1, D_2 and D_3, we assume that:

1) The domain D_1 corresponds to the upper part of the glass jet for $z_0 = 0 \leqslant z \leqslant z_1$. The flow is fully two-dimensional in the meridian plane Eq. (5.1).

2) The domain D_2 is the one-dimensional region investigated by Glicksman et al. The axial velocity component is

$$v = w(z). \tag{5.2}$$

3) The domain D_3 is the solid flow region corresponding to the constant diameter of the fiber:

$$\mathbf{V} = V_2 \mathbf{e}'_z, \tag{5.3}$$

V_2 is the drawing rate.

For the determination of the section z_1, at which the one-dimensional region D_2 begins, we use GLICKSMAN'S hypothesis [3] according to which z_1 is the section where the absolute value of the slope of the free surface is less than one-tenth. For the glass jet, the section z_1 was found to be between $2R_0$ and $5R_0$, where R_0 denotes the radius of the nozzle. The section z_2 was found to be, according to our experiments, between $15R_0$ and $20R_0$.

5.1. General assumptions

In our theoretical study of the glass flow problems, we made the following assumptions.

1) The glass is considered as a Newtonian liquid of temperature-dependent viscosity $\mu(T)$. This viscosity can be approximated by piecewise polynomial functions of T.

2) The jet surface can be represented by the following equation:

$$R(z) = R_0 \exp[\bar{a}z^2 + \bar{b}z], \tag{5.4}$$

where a and b are constants calculated from the experimental data of the free surface by a least-squares technique. The agreement of experimental and theoretical data is obtained within 3%.

3) From the incompressibility of glass, we can use, in the axisymmetric case, a stream function $H(\varrho, z)$ such that:

$$u = \frac{1}{\varrho}\frac{\partial H}{\partial z} \tag{5.5}_1$$

and

$$v = -\frac{1}{\varrho}\frac{\partial H}{\partial \varrho}. \tag{5.5}_2$$

The streamlines are assumed to have the same analytical expression as the free surface:

$$\varrho = \varrho_0 \exp[az^2 + bz], \tag{5.6}$$

where a and b are parameters depending on the streamline. ϱ_0 is the radial coordinate at the exit section $z = z_0 = 0$.

5.2. Kinematics

Let z_3 be a section of region D_2 where the velocity is known, and V_3 the constant velocity at the cross-section (Fig. 4). We can express the stream function $H(\varrho, z)$ with the parameter r_3, the radial coordinate at section z_3. R_3 is the fiber radius at $z = z_3$.

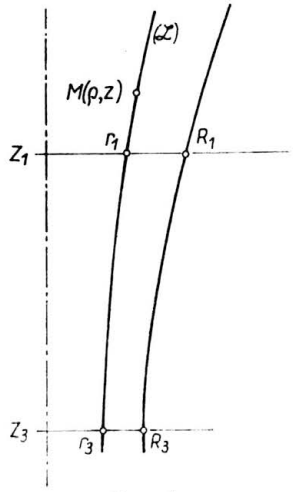

FIG. 4.

According to the stream function description, we have

$$\forall(\varrho, z) \in \mathscr{L}, \quad H(\varrho, z) = G(r_3) = \text{constant}, \tag{5.7}$$

V_3 is konwn and, for every point $M(\varrho, z)$ such that $z < z_3$, there exists a unique value $r_3 \in [0, R_3]$ such that

$$H(\varrho, z) = G(r_3) = -\frac{Q(r_3)}{2\pi} = -(r_3)^2 \frac{V_3}{2}, \tag{5.8}$$

where $Q(r_3)$ denotes the volume flow rate related to the section z_3 of radius r_3 (Fig. 4).

A particular case is given by $z_3 = z_2$. Then V_3 is the drawing rate.

Now, using r_3 as a parameter for the streamlines, Eq. (5.6) becomes

$$\varrho = r_3 \exp[a_{r_3}(z^2 - z_3^2) + b_{r_3}(z - z_3)]. \tag{5.9}$$

The symbols a_{r_3} and b_{r_3} indicate the dependence on parameter r_3.

We assume that the coefficient b is in the form

$$b_{r_3} = k(r_3)^2. \tag{5.10}$$

Since

$$\bar{b} = b_{R_3}, \tag{5.11}$$

k is known by Eqs. (5.10) and (5.11).

We also have

$$\bar{a} = a_{R_3}.$$

Then the kinematics can be completely determined under the assumption of Eq. (5.10).

Let V_1 be the axial velocity for $z = z_1$. The conservation of the volume flow rate Q gives us

$$Q = \pi R^2(z) w(z) = \pi (R_1)^2 V_1 = \pi (R_3)^2 V_3. \tag{5.12}$$

For every r_3, $r_3 \in [0, R_3]$, there exists a unique value $r_1 \in [0, R_1]$ such that

$$(r_1)^2 V_1 = (r_3)^2 V_3. \tag{5.13}$$

From Eq. (5.9) we obtain

$$r_1 = r_3 \exp[a_{r_3}(z_1^2 - z_3^2) + b_{r_3}(z_1 - z_3)] \tag{5.14}$$

and combining Eqs. (5.13) and (5.14), we have

$$a_{r_3} = \frac{1}{z_1^2 - z_3^2}\left[\ln \sqrt{\frac{V_3}{V_1}} - b_{r_3}(z_1 - z_3)\right]. \tag{5.15}$$

The derivatives of a_{r_3} are expressed as

$$a'_{r_3} = -b'_{r_3}/(z_1 + z_3), \tag{5.16}$$

$$a''_{r_3} = -b''_{r_3}/(z_1 + z_3), \tag{5.17}$$

$$a'''_{r_3} = b'''_{r_3} = 0. \tag{5.18}$$

Next, we consider the transformation which associates the sets of variables (ϱ, z) and (r_3, ζ) by the following equations:

$$\begin{aligned} z &= \zeta, \\ \varrho &= f(r_3, \zeta) = r_3 \exp[a_{r_3}(\zeta^2 - z_3^2) + b_{r_3}(\zeta - z_3)]. \end{aligned} \tag{5.19}$$

Using Eqs. (5.8), (5.9) and (5.15), (5.16), (5.17), (5.18) we can compute the velocities and their first and second spatial derivatives in the upper region D_1, in an analytical form.

For $z_0 \leqslant z \leqslant z_1$, we have for the velocities:

$$V(\varrho, z) = V_3 \exp[-a_{r_3}(z^2 - z_3^2) - b_{r_3}(z - z_3)] \frac{\partial r_3}{\partial \varrho} \tag{5.20}$$

with

$$\frac{\partial r_3}{\partial \varrho} = \frac{\exp[-a_{r_3}(z^2 - z_3^2) - b_{r_3}(z - z_3)]}{1 + r_2[a'_{r_3}(z^2 - z_3^2) + b'_{r_3}(z - z_3)]} \tag{5.21}$$

and

$$u(\varrho, z) = (2az + b)\exp[-a_{r_3}(z^2 - z_3^2) - b_{r_3}(z - z_3)] v(\varrho, z). \tag{5.22}$$

5.3. Navier–Stokes equations and boundary conditions in region D_1

The dynamical equations are written in the upper region, in cylindrical coordinates, the body forces being neglected:

$$\frac{\partial p}{\partial \varrho} = \mu\left[\frac{\partial^2 u}{\partial \varrho^2} + \frac{1}{\varrho}\frac{\partial u}{\partial \varrho} - \frac{u}{\varrho^2} + \frac{\partial^2 u}{\partial z^2}\right] + 2\frac{\partial \mu}{\partial \varrho} + \frac{\partial u}{\partial \varrho} + \frac{\partial \mu}{\partial z}\left(\frac{\partial v}{\partial \varrho} + \frac{\partial u}{\partial z}\right), \tag{5.23}$$

$$\frac{\partial p}{\partial z} = \mu\left[\frac{\partial^2 v}{\partial \varrho^2} + \frac{1}{\varrho}\frac{\partial v}{\partial \varrho} + \frac{\partial^2 v}{\partial z^2}\right] + 2\frac{\partial \mu}{\partial z}\frac{\partial v}{\partial \varrho} + \frac{\partial \mu}{\partial \varrho}\left(\frac{\partial v}{\partial \varrho} + \frac{\partial u}{\partial z}\right). \tag{5.24}$$

The boundary conditions at the interface between the glass and the surrounding air are obtained by writing the equality of normal and tangential stresses:

$$p(R, z)(1 + R'_z) + 2\mu(R, z)\left[-\frac{\partial u}{\partial \varrho} + R'_{(z)}\left(\frac{\partial u}{\partial z} + \frac{\partial v}{\partial \varrho}\right) - R'^2_{(z)}\frac{\partial v}{\partial z}\right] = (1 + R'_z)\left[P_a + \gamma_T\left(\frac{1}{\Gamma} + \frac{1}{\Gamma_1}\right)\right] \tag{5.25}$$

in the normal direction $\mathbf{n}$ (Fig. 4), and

$$\mu(R, z)\left[\left(\frac{\partial u}{\partial z} + \frac{\partial v}{\partial \varrho}\right)(1 - R'^2_z) + R'_z\left(\frac{\partial u}{\partial \varrho} - \frac{\partial v}{\partial z}\right)\right] = (1 + R'^2_z)\left[\tau_a + \frac{\partial \gamma_T}{\partial z}\cos\varphi\right] \tag{5.26}$$

in the tangential direction $\boldsymbol{\tau}$.

P_a denotes the pressure in the air, τ_a is the drag component of the air, $p(R, z)$ is the pressure at the glass surface, Γ and Γ_1 are the radii of curvature of the free surface given by

$$\frac{1}{\Gamma} = \frac{\cos\varphi}{R(z)} \quad \text{and} \quad \Gamma_1 = \frac{-(1 + R'^2_z)^{3/2}}{R''_{(z)}}. \tag{5.27}$$

For Eqs. (5.23), (5.24), (5.25) and (5.26), the known quantities are:

the kinematic quantities;

the viscosity $\mu(R, z)$ calculated from temperature measurements;

the temperatures T_0 and T_1, the pressures p_0 and p_1 at the sections z_0 and z, respectively, which are assumed to be a constant.

Then,

$$\begin{aligned} &\mu(\varrho_0, z_0) = \mu_0, \\ &p(\varrho_0, z_0) = p_0, \quad \varrho_0 \in [0, R_0], \end{aligned} \tag{5.28}$$

$$\begin{aligned} &\mu(r_1, z_1) = \mu_1, \\ &p(r_1, z_1) = p_1, \quad r_1 \in [0, R_1]. \end{aligned} \tag{5.29}$$

From these considerations, the quantities to be determined are:

$p(R, z)$, pressure at the free surface;

$p(\varrho, z)$, $\mu(\varrho, z)$ pressure and viscosity inside the jet;

$p_a(R, z)$, $\tau_a(R, z)$.

The Navier–Stokes equations (5.23) and (5.24) can be written in the following forms:

$$\frac{\partial p}{\partial \varrho} = A_1\mu + \frac{\partial \mu}{\partial \varrho}B_1 + \frac{\partial \mu}{\partial z}C_1, \tag{5.30}$$

$$\frac{\partial p}{\partial z} = A_2\mu + \frac{\partial \mu}{\partial z}B_2 + \frac{\partial \mu}{\partial \varrho}C_2. \tag{5.31}$$

The quantities A_1, B_1, C_1, A_2, B_2, C_2 are known from the kinematics.

Equation (5.26) gives directly the unknown τ_a. Equation (5.25) is used together with the Navier–Stokes equations.

5.4. Numerical solution

Because of the possibility of non-negligible errors in estimating the partial derivatives of μ and p on the irregular mesh build on the streamlines (due to the rapid attenuation of the glass jet), we transform the physical domain D_1 into a rectangular domain D_1' by using Eqs. (5.19). Then the derivation operators can be written as

$$\frac{\partial}{\partial \varrho} = \frac{1}{f'_{r_3}} \frac{\partial}{\partial r_3}, \tag{5.32}$$

$$\frac{\partial}{\partial z} = \frac{\partial}{\partial \zeta} - \frac{f'_\zeta}{f'_{r_3}} \frac{\partial}{\partial r_3}. \tag{5.33}$$

The Navier–Stokes equations and the boundary conditions (5.25) are solved in domain D_1' (Fig. 5) which is discretized with indices i (streamlines) and j (sections on the streamlines). On the rectangular mesh, we use classical difference formulae for the derivatives.

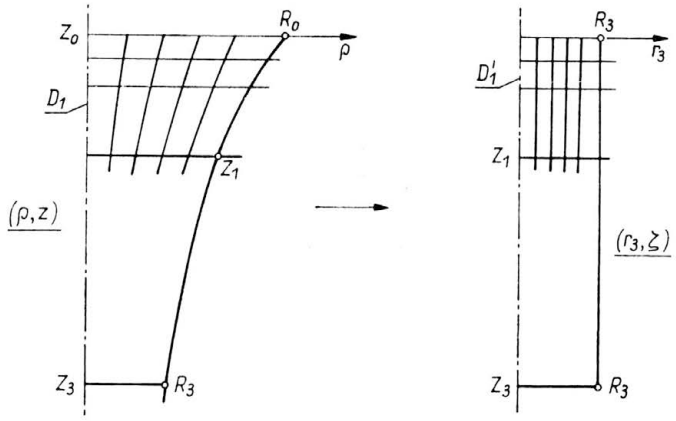

FIG. 5. Transformation of domain D_1 into D_1' (rectangular).

Concerning the balance of equations and unknowns, we define the mesh as

$$(I, J) \in N, \quad I \in [1, I_0], \quad J \in [s, J_0],$$

$I = 1$ for the free surface and $I = I_0$ on the centreline, $J = 1$ for the section $z = z_0 = 0$, $J = J_0$ for $z = z_1$.

The sections z_0 and z_1 are not considered. We have $J_0 - 2$ equations for the boundary equation (5.25), $2(J_0 - 2)(I_0 - 1)$ Navier Stokes equations for $I \in [1, I_0 - 1]$, $J_0 - 2$ equations on the axis (the first Navier–Stokes equation (5.30) vanishes).

This leads to the total number of $2(J_0 - 2)I_0$ equations

For the unknowns we obtain

$J_0 - 2$ unknowns for P_a,

$I_0(\varepsilon - 2)$ unknowns for p,

$(I_0 - 1)(J_0 - 2)$ unknowns for μ.

So we get the same number of unknowns and the equations: $2I_0(J_0 - 2)$.

5.5. Numerical results

The numerical technique was carried out for different drawing conditions: $V_2 = 3.2$, 8.7, 11.3, 15, 18.1 m/s and temperatures at the jet surface. The results of kinematics (Fig. 6) are for the drawing rate of 15 m/s. In that case the section z_1 was found to be 0.405 cm (about four radii downstream the exit section) and the section z_2 was at 16.5 cm (16.5 radii).

In Fig. 7, we show the evolution of the streamlines in the jet from the exit section $z_0 = 0$, which indicate the rapid attenuation of the fiber diameter.

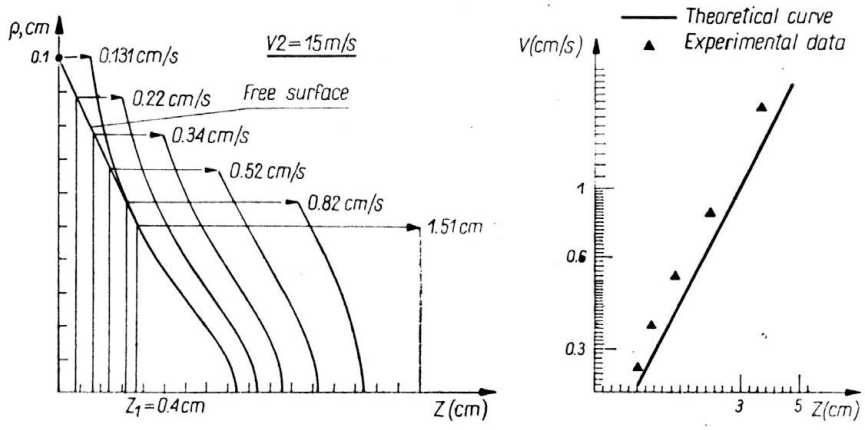

FIG. 6. Kinematic results in the glass jet.

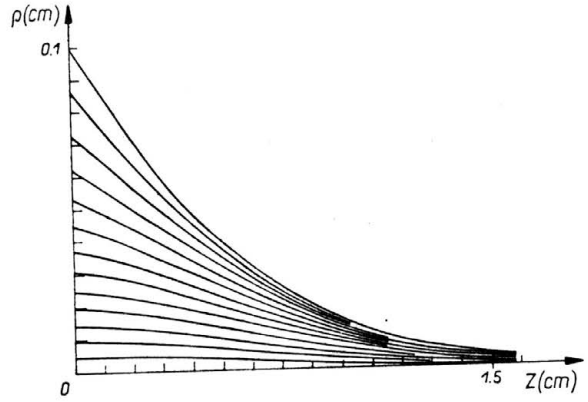

FIG. 7. Streamlines in the glass jet.

For $V_2 = 15$ m/s, we give in Fig. 8 the computed values of temperature inside the upper region D_1. The results show that:

1) Inside the jet, the temperature is higher than at the free surface. This fact is quite acceptable from a physical point of view.

2) Apart from the limit sections z_0 and z_1, the temperature variation in a cross-section of the jet is not negligible.

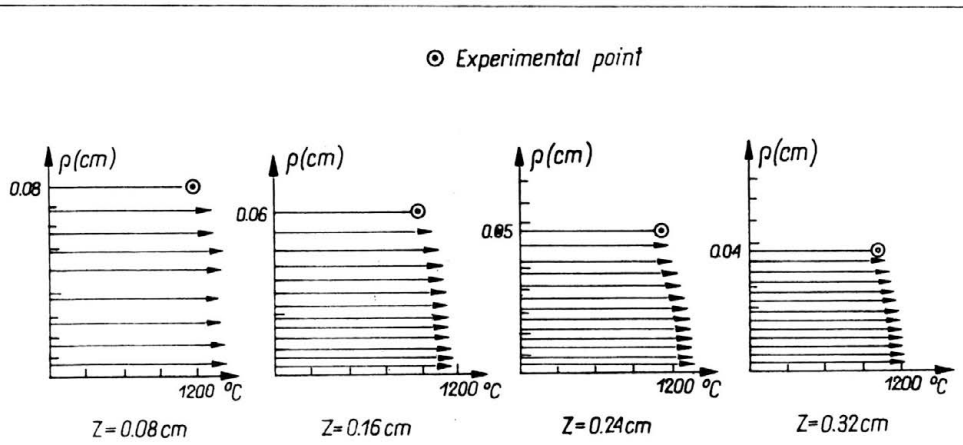

FIG. 8. Computed values of temperature in region D_1.

The same comments can be made concerning the other drawing conditions.

Apart from the computation of the temperature field inside the jet we performed tests on stability by slightly changing the boundary conditions for temperature. The tests on the sensitivity of the boundary conditions for temperature led to minimization of the temperature variation for a cross-section when the free surface temperatures of the jet T_{SL} were given by

$$T_{SL} = T_{exp} + 20 \text{ C},$$

where T_{exp} is the measured temperature. This result, which was found for different drawing conditions clearly indicates, the importance of thermal conditions in the glass spinning process.

6. Heat transfer model under drawing conditions

6.1. Four constants models for the radiative transfer

As we pointed out, it is highly difficult to propose a realistic equation for the radiative heat transfer inside the glass under the spinning conditions. We propose in the following a method for the determination of the radiative flux vector $\mathbf{q}_r$ by using experimental and numerical results of our kinematic and dynamical model. Indeed, by considering the energy equation

$$\nabla \mathbf{q}_r = \lambda_c \left[\frac{\partial^2 T}{\partial \varrho^2} + \frac{1}{\varrho} \frac{\partial T}{\partial \varrho} + \frac{\partial^2 T}{\partial z^2} \right] - \varrho C_p \left[u \frac{\partial T}{\partial \varrho} + v \frac{\partial T}{\partial z} \right] = A_0, \tag{6.1}$$

the right-hand side of this equation contains only known quantities (temperature, kinematics); C_p denotes the specific heat coefficient, λ_c the thermal conductivity coefficient.

Then we make the following assumption:

The radiative flux vector $\mathbf{q}_r(\varrho, z)$ is given by

$$\mathbf{q}_r = q_\varrho(\varrho, z)\mathbf{e}'_\varrho + q_z(\varrho, z)\mathbf{e}'_z, \tag{6.2}$$

with

$$q_\varrho(\varrho, z) = a_0 \varrho^3 z^3 + a_1 \varrho z^2, \tag{6.3}$$

$$q_z(\varrho, z) = a_2 \varrho^2 z^2 + a_3 \varrho^2 z, \tag{6.4}$$

where a_0, a_1, a_2, a_3 are four constants to be determined.

Since

$$\nabla \mathbf{q}_r(\varrho, z) = A_0 = \frac{\partial q_\varrho}{\partial \varrho} + \frac{\partial q_z}{\partial z} + \frac{q_\varrho}{\varrho}, \tag{6.5}$$

we can express the operator ∇q_r in variables (r_3, ζ) by

$$\nabla \overline{q}_r'(\varrho, z) = \frac{1}{f_{r_3}'} \frac{\partial q_\varrho}{\partial r_3} + \frac{\partial q_\zeta}{\partial \zeta} - \frac{f_\zeta'}{f_{r_3}'} \frac{\partial q_\zeta}{\partial r_3} + \frac{qp}{\varrho}, \tag{6.6}$$

which gives the following form:

$$\nabla \mathbf{q}_r(\varrho, z) = a_0 \alpha_0 + a_1 \alpha_1 + a_2 \alpha_2 + a_3 \alpha_3. \tag{6.7}$$

The four constants (α_0, α_1, α_2, α_3 are known) are computed by using a least squares technique. We consider the expressions

$$E = \sum_{i=2}^{J_0} \sum_{J=1}^{J} [a_0 \alpha_{0(J,I)} + a_1(\alpha_{1(J,I)} + a_2 \alpha_{2(J,I)} + a_3 \alpha_{3(J,I)} - A_{0(J,I)}]^2, \tag{6.8}$$

from which the four constants a_0, a_1, a_2, a_3 are determined by the equations

$$\frac{\partial E}{\partial a_k} = 0, \quad k = 0, 1, 2, 3. \tag{6.9}$$

These equations are linear in terms of a_k.

The approximation of the radiative flux vector by the four-constant model leads to 50% accuracy for the quantity

$$\frac{\nabla \mathbf{q}_r - A_0}{A_0}. \tag{6.10}$$

It is to be pointed out that $\nabla \mathbf{q}_r$ values from the Rosseland equation given by Eqs. (2.3) and (2.6) were found to be by 4 orders of magnitude greater than A_0.

6.2. Convective heat transfer coefficient

When considering thermal exchanges in the glass jet, the exchange between the jet surface and the surroundings (air) is to be investigated separately from the interior of the jet.

The energy equation at the jet surface is given by

$$-K_g \frac{\partial T}{\partial n} = h(z) \cdot (T - T_\infty) + q_\varrho(\varrho, z) \cos\varphi + q_z(\varrho, z) \sin\varphi, \tag{6.11}$$

where K_g denotes the thermal conductivity of the glass, $h(z)$ is the convective heat transfer coefficient at the jet surface, T_∞ a reference temperature, q_ϱ and q_z are the components of the radiative flux vector, φ is the angle between the normal vector n to the surface and the axis ϱ.

For the calculation of $h(z)$, we assume that the radiative flux vector at the jet surface is given by the four constants a_0, a_1, a_2 and a_3.

Then $q_\varrho(\varrho, z)$ and $q_z(\varrho, z)$ are known at the free surface.

In Eq. (6.11), the only unknown quantity is $h(z)$.

The results of the computation of the convective heat transfer coefficient are given in Fig. 9. The values of this coefficient are quite acceptable from a physical point of view.

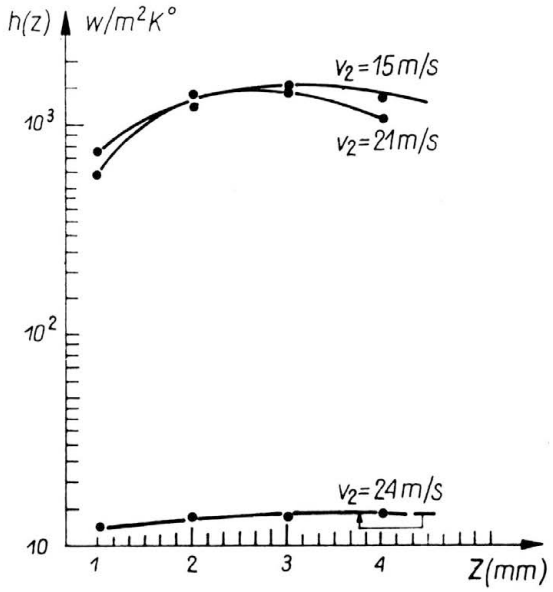

FIG. 9. Convective heat transfer coefficient versus the drawing rate.

7. Conclusion

In the present paper we have considered the upper jet region of the glass jet during the glass spinning process. Two theoretical models have been set up. The first model concerns the use of experimental data of temperature and velocities in the Navier–Stokes equations in order to determine the temperature field in the upper jet region. This technique avoids taking into account the complicated radiation problem involved in the glass extrusion. The numerical results are consistent with the phenomenology of the fiber process and have shown the sensitivity of the thermal conditions around the glass jet. The second model is related to the modelization of the radiative transfer using the results of the kinematic model. The so-called "four constant model" has given acceptable results for the approximation of the radiative flux vector $\mathbf{q}_r$. Moreover, this model has permitted us to estimate a convective transfer coefficient h between the glass and its surroundings. The computed data of the coefficient h have a correct order of magnitude. According to these results, the parameters of the radiation heat transfer and the convective transfer coefficients can be included in a more complete analysis of the glass spinning problem, which would involve simultaneously the conservation laws of mass, momentum and energy.

Acknowledgments

The authors would like to express their gratitude to the Saint Gobain Company for numerous helpful discussions (the data of viscosity of the *E*-glass were obtained from this source) and Disa Electronics, France, for their help in the use of the Argon-laser equipment for the velocity measurements in glass at high temperatures.

References

1. H. OZISIK, *Radiative transfer and interactions with conduction and convection*, J. Wiley and Sons 1973.
2. SAINT GOBAIN, Internal Report, 1982.
3. L. R. GLICKSMAN, *The dynamics of heated free jet of variable viscosity liquid at low Reynolds numbers*, J. Am. Soc. Mech. Engrs. **90D**, 343–354, 1968.
4. L. R. GLICKSMAN, S. KRISHNAN, *A two-dimensional analysis of heated free jet at low Roynolds numbers*, J. Am. Soc. Mech. Engrs., **93D**, 355–364, 1971.
5. L. R. GLICKSMAN, *A prediction of the upper temperature limit for glass fibre spinning*, Glass Technology **15**, 1, 16–20, 1974.
6. B. CASWELL and R. SAYLES, *A finite element analysis of the upper jet region of a fiber drawing flow field*, Division of Engineering Brown University, Providence R. I. (Report NSF — 18421/1) December 1981.
7. H. STEHLE and R. BRUCKNER, *Simultaneous rheological and thermal analysis of glass fiber drawing. Part* 1. *Solution of the coupled differential equations*, (Simultane rheologische und thermische Analyse des Glasfaserziehvorganges. Teil 1. Lösung der gekoppelten Differentialgleichungen und Stoffwerte). Glastechn. Ber., **52**, 4, 82–91, 1979.
8. H. STEHLE and R. BRUCKNER, *Simultaneous rheological and thermal analysis of the glass fiber drawing process. Part 2. Numerical results and comparison with experiments* (Simultane rheologische und thermische Analyse des Glasfaserziehvorganges. Teil 2. Numerische Ergebnisse und Vergleich mit den Experimenten), Glastechn. Ber., **52**, 5, 105–115, 1979.
9. B. P. HUYNH, R. I. TANNER, *Study of the non-isothermal glass fibre drawing process*, Rheol. Acta., 22, 482–499, 1983.

INSTITUT DE MECANIQUE DE GRENOBLE, FRANCE.
LABORATOIRE ASSOCIÉ AU CNRS, GRENOBLE, FRANCE.

Received April 2, 1985.